Tutor/s

Dra. Anna De Juan Capdevila

Departament d'Enginyeria Química i Química Analítica

Dra. Laura Tositti

Dipartimento di Chimica dell'ambiente e dei beni culturali

Grau de Química

Treball Final de Grau

Set up and optimization of an integrated multi-instrumental method for analysing Saharan dust in atmospheric PM filters from Sierra Nevada
Configuració i optimització d'un mètode multi-instrumental integrat per analitzar pols sahariana en filtres d'aerosol atmosfèric de la Sierra Nevada

Josep Mestres Sanna

January 2019

UNIVERSITAT DE BARCELONA

B:KC Barcelona Knowledge Campus
Campus d'Excel·lència Internacional

"Considerate la vostra semenza:

fatti non foste a viver come bruti

ma per seguir virtute e canoscenza"

Dante Alighieri

En primer lloc voldria donar les gràcies a la Dr. Laura Tositti, per haver-me acollit "all'Università di Bologna" i deixar-me treballar durant els mesos d'Erasmus al seu laboratori. També a la meva tutora a distància, l'Anna de Juan, que s'ha mostrat accessible i disposada a ajudar-me tot i la distància sempre que ho he necessitat.

Tota la feina feta hauria estat impossible sense la constant ajuda de'n Pietro, amb qui, a més de durs moments de feina he pogut compartir moments molt divertits, i probablement, hagi sigut la persona amb qui més cafès per hora he pres a la meva vida.

Com és degut, ni aquest Erasmus, ni aquest graduat haurien estat possibles sense els meus pares, i la resta de la família, que m'han ajudat i recolzat en tot moment (i que m'han finançat el grau, tot i l'alt preu de les Universitats Públiques Catalanes).

Arribats a aquest punt només em falta donar les gràcies a les persones que, sense citar el seu nom, saben que han fet d'aquest Erasmus el millor final de carrera possible, a tots vosaltres, moltes gràcies, també a tota la gent fantàstica que he conegut durant el curs d'aquesta carrera universitària.

REPORT

Contents

1. SUMMARY

This report is the union of some of the work and analyses carried out at the Laboratory of Dra. Laura Tositti, Bologna University. It is based on the analyses of Particulate Matter, one of the main atmospheric pollutants which is able to cause serious health and environmental problems. Specifically, the sampling of analysed filters has been done at Sierra Nevada, south of Spain, within the Spanish research project FRESA. This sampling station has the characteristic of being next to North Africa at a high altitude (2550 m a.s.l.). Because of this, Particulate Matter collected in these filters often includes Saharan Dust that comes from North Africa transported by the wind. This kind of Particulate Matter has a specific chemical and physical composition. It is made mostly of coarse particulate and its colour tends to be reddish because of its content in iron oxides such as hematite.

The aim of this report is to use a series of basic and widely available spectroscopic techniques to analyse these filters in order to characterise in detail the properties and composition of airborne particulate matter. Then the idea was to develop a quantitative analytical approach from spectroscopic techniques usually applied only in a qualitative way according to an approach partly experimental and partly chemometric recently introduced at Dra. Tositti's lab.

Portions of a series of 19 weekly filters from Sierra Nevada were analysed in triplicate. Experimental procedures and data analyses will be separated in 5 parts each. These parts are the 4 analyses of the filters that has been done: Homogeneity test, UV-VIS Diffuse Reflectance Spectroscopy (UV-VIS DRS), Fourier Transform Infrared

Spectroscopy with attenuated total reflection (FT-IR ATR), and Chemiluminescence using a Luminol-based test for the detection of ROS (Reactive Oxygen Species).

Moreover, a parallel work of this thesis was the design and optimization of the resuspension system, a special assembly that was set up to produce solid calibration standards on filters in order to quantify chemical compounds on the filters, (especially hematite). This work therefore enabled the acquisition of several properties of these environmental samples, i.e. the filters weight and their homogeneity, spectroscopic signal of hematite and colour information, and IR bands that mostly explain the quartz and hematite composition, along with others, and finally, chemiluminescence maximum peak.

All the data obtained in this thesis work was finally subjected to Spearman correlation analysis extending my dataset to data previously obtained at Bologna lab such as Ion Chromatography as well as meteorological data during the sampling period. A high correlation was found between hematite, PM_{10}, reddish colour of filters, and the IR absorption band, while chemiluminescence seems to be correlated with acetate and calcium cation.

Key words: Particulate Matter, Saharan dust, spectroscopy, deposition, coarse granulometry, hematite, quartz, filters, Principal Component Analysis (PCA), pre-processing data, Spearman correlation, homogeneity, colorimetric space.

2. RESUM

Aquest informe és la unió del resultat de les tasques i de les anàlisis realitzats al Laboratori de Dra. Laura Tositti, Universitat de Bolonya. Es basa en les anàlisis d'aerosol atmosfèric, un dels principals contaminants atmosfèrics capaços de causar problemes greus de salut i medi ambient. En concret, la mostra de filtres analitzats s'ha realitzat a Sierra Nevada, Andalusia, dins del projecte de recerca espanyol FRESA. Aquesta estació de mostreig té la característica de ser al costat del Nord d'Àfrica a gran alçada (2550 m a.s.l.). A causa d'això, l'aerosol atmosfèric recollit en aquests filtres sovint inclou pols sahariana que prové del nord d'Àfrica transportada pel vent. Aquest tipus aerosol atmosfèric té una composició química i física específica. Està constituïda majoritàriament de partícules gruixudes i el seu color tendeix a ser vermellós a causa del seu contingut en òxids de ferro com l'hematita.

L'objectiu d'aquest informe és d'utilitzar una sèrie de tècniques espectroscòpiques bàsiques i àmpliament disponibles per tal d'analitzar aquests filtres i caracteritzar detalladament les propietats i la composició de les partícules aerotransportades. Posteriorment, la idea era de desenvolupar un enfocament analític quantitatiu a partir de tècniques espectroscòpiques normalment aplicades només de manera qualitativa segons un enfocament parcialment experimental i en part quimiomètric recentment presentat al Laboratori de la Dra. Tositti.

Parts d'una sèrie de 19 filtres setmanals procedents de Sierra Nevada han estat analitzades per triplicat. Els procediments experimentals i les anàlisis de dades se separaran en 5 parts cadascuna. Aquestes peces són les 5 anàlisis dels filtres que s'han realitzat: sistema de resuspensió, prova d'homogeneïtat, espectroscòpia en reflectància UV-Vis, Espectrofotòmetria transformada de Fourier FTIR en mode ATR

(reflectància total atenuada) i la quimioluminescència mitjançant una prova basada en Luminol per a la detecció de ROS (espècies reactives d'oxigen).

Aquest treball permet, per tant, l'adquisició de diverses propietats d'aquestes mostres ambientals, és a dir, el pes dels filtres i la seva homogeneïtat, el senyal espectroscòpic d'hematita i la informació del color i les bandes d'infrarojos que expliquen principalment la composició de quars i hematites, juntament amb d'altres, i finalment, quimioluminescència al pic màxim. Pel que fa al sistema de resuspensió, s'ha establert un assemblatge especial per tal de produir estàndards de calibratge sòlids en filtres per quantificar els compostos químics en els filtres, en aquest cas l'hematita. En particular, amb el sistema de resuspensió, s'ha pogut produir un filtre homogeni d'hematita pura per utilitzar-lo provisionalment com a estàndard per a l'espectroscòpia IR qualitativa.

Finalment, totes les dades obtingudes en aquest treball de tesi han estat sotmeses a una anàlisi de correlació de Spearman que ampliava el meu conjunt de dades a dades prèviament obtingudes al laboratori de Bolonya, com ara la cromatografia iònica i les dades meteorològiques durant el període de mostreig. Es va trobar una alta correlació entre hematita, PM_{10}, Cab * (en aquest cas, correlació inversa) i la banda d'absorció de l'IR, mentre que la quimioluminescència només es correlaciona amb acetat i catió de calci relacionats amb la contaminació antropogènica.

Paraules clau: Aerosol atmosfèric, pols sahariana, espectroscòpia, deposició, granulometria gruixuda, hematita, quars, filtres, Anàlisi de Components Principals) PCA, pretractament de dades, correlació de Spearman, homogeneïtat, espai colorimètric.

3. INTRODUCTION

3.1 Particulate Matter

Particulate Matter (usually shortened to PM) is defined as a suspension of particles in a gaseous medium, i.e. the atmosphere. PM size ranges between few nanometres and hundreds of micrometres[1].

PM consists of a wide range of different and complex particles that can be solid or liquid or both according to hygroscopicity, and which can vary in source, size, shape and chemical composition.

Another way to classify Particulate Matter is taking in consideration its sources. Depending on it, the particulate can be natural or anthropogenic. If PM comes directly from the source without changing its chemical composition, it is called primary PM. Instead, if it is produced by oxidative reactions (atmosphere is oxidant) with gases that are first emitted to the atmosphere and subsequently undergo gas-to-particle conversion mainly driven by photochemical processes, it is defined as secondary. The atmosphere is the PM's means of transportation so, during this transportation the particulate can be subjected to physical/chemical changes due to collisions with other particles or other substances (gases and vapours) in the atmosphere under the influence of solar radiation as the source of energy for the reactions. This is the source of a continuous variation in the physical characteristics, chemical composition and distribution of the PM. the reason why PM is sampled and analysed is to assess its origin through high definition chemical analysis (known as PM chemical speciation) leading to identification of its origin and of

the possible effects on human health. Specifically, the detailed analysis of time series data of PM gives us great information about the circulation and the quality of the air we breathe and also to its influence on climate change.

Moreover, it is important to know that PM can have important effects both on the environment and on human health. It interacts with the environment as a pollutant by causing problems like altering the radiation balance of the Earth, catalysing the destruction of ozone in the stratosphere[2], affecting cloud formation processes, contributing to global warming or even reducing the visibility[3]. Regarding the effect on the human health, the main problem is that fine and ultrafine particles can penetrate the respiratory systems reaching the alveoli so causing several health problems such as for example respiratory, cardiovascular[4] and neurological diseases by means of oxidative stress. Residing in areas with high levels of particulate matter has also been associated with greater cardiovascular disease incidence and mortality[5]. For all these reasons we can understand why it is so important to study this pollutant.

3.1.1 Size and geometry of Particulate Matter

Particulate size influences in 2 fundamental aspects[1]:

- Access into the body.
- Medium residence time of the particles in the atmosphere.

For these reasons it is important to define accurately the diameter of the PM. Usually the shape of PM is not regular; it is rarely spherical, and its density is function of composition. Therefore, **Aerodynamic diameter (D_a)** is the diameter of a particulate whose terminal velocity is the same as a sphere whose density is 1g/cm^3 [6].

Once it has been defined the diameter of the particulate, it is easier to classify the kinds of particulate as a function of its size:

- **Coarse PM:** 100 µm ≥ D_a > 1 µm
- **Fine PM:** 1 µm ≥ D_a > 0.1 µm

- **Ultrafine PM:** $D_a \leq 0.1$ µm

This means in practice that aerosol particles range from 1 nm up to several tens of µm spanning therefore more than 4 orders of magnitude. As a general rule PM_x is the general name to be used, where X is the uppermost size of the particles sampled with a given device.

$PM_{2,5}$ is known to be mostly secondary and anthropic instead $PM_{10-2,5}$ can come from natural sources like Saharan dust (explained in point 3.2.3.)

3.1.2 Formation process

There is a close relationship between particle size and particle formation processes[3]. It was found that particles have a complex size distribution made of 4 main modes (polydisperse system). associated with the granulometry and the process the particles present:

- **Nucleation Mode** (10-12nm): They are formed after gases that with reaction/condensation (or gas-to-particle) process change from free molecule state to aggregates of particles (clusters), and finally become particles with a preferred size.
- **Aitken Mode** (70-80nm): They are formed by collision/coagulation of particles previously formed and they can subsequently increase in size by condensation of gases on their surface.
- **Accumulation mode** (300-700nm): They are created by collision, coagulation or coalescence of the particles formed by the previous formation process. **Coarse mode** (D_a>1µm): usually they come from erosion or mechanic abrasion of rocks and evaporation of seawater processes. It is not connected with the rest of formation modes[1].

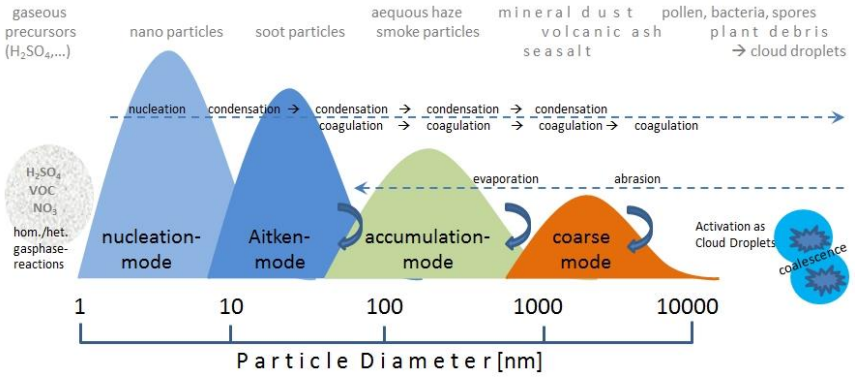

Figure 3.1 PM size distribution, relation between number density (particles/Volume), particle size and formation processes[7].

3.1.3 Sources and chemical compounds

Sources can be classified as natural or anthropic. Usually natural sources are processes working at low temperatures. Instead, anthropic sources use to be at high temperatures[8].

- **Natural Sources**

- **Marine spray** expelled out from the ocean or seas as a result of the interaction between waves and wind. This kind of PM is formed when the droplets on the ocean surface explode releasing salts or other chemical compounds dissolved in the water. The diameter of these PM can vary, as it can goes from 0,2 to 200 μm. However, most of them are included between 2-20 μm. The main compounds are: sodium (Na), chlorine (Cl), and in lower concentrations cadmium (Cd), zinc (Zn), Cobalt (Co), etc. complexed with organic substances.

- **Volcanic emissions** are made of gases and PM material both primary and secondary origin. Emitted dust can reach upper layers of the troposphere, and even the stratosphere. Consequently, they have a long time of residence in the atmosphere that can even reach a year.

- **Biosphere** is the origin of organic substances either as primary sources like carbon dioxide (CO_2) or as many complex substances (like volatile organic compounds (VOCs), spores, pollen, etc., the latter components of aerosol as well) produced by living organisms or CH_4 and ash produced by wildfires. Some of the most important compounds produced by this source are sulphate (SO_4^{2-}), nitrate (NO_3^-) and ammonium (NH_4^+), produced also by anthropogenic sources.

- An important source of natural PM is the **Earth's crust**. Because of the effect of mechanical erosion process or other physico-chemical processes lithogenic material can be eroded from the rocks and soil, resuspended and transported by the wind. Depending on the substrate it comes from, the chemical composition is a function of the rock type it comes from, but usually consists of: aluminium (Al), silicon (Si) and Iron (Fe), etc.[9]. In arid or semi-arid zones this phenomenon gets more significant as the surface is more erodible. If the wind is strong in these zones, a dust-storm can lift the particles, and carry them through long distances. In the Mediterranean area, in North Africa, these phenomena are quite frequent as the weather conditions encourage it. This dust is called Saharan Dust (SD), and is the focus of this work.

- **Anthropogenic Sources**

- Anthropogenic sources contribute in global PM is less than the natural contribute. However, in urban areas, the anthropogenic PM has the biggest fraction. Most of anthropogenic sources of particulate come from combustion process, that can be distinguished between stationary sources (industrial activity and heating sources) or dynamic sources (modes of transport). Carbon and sulphur are the main compounds in all these emissions[10]. In addition, nickel (Ni), vanadium (V), or copper (Cu) and bromine (Br), chloride (Cl), potassium (K), and Pb can be found.

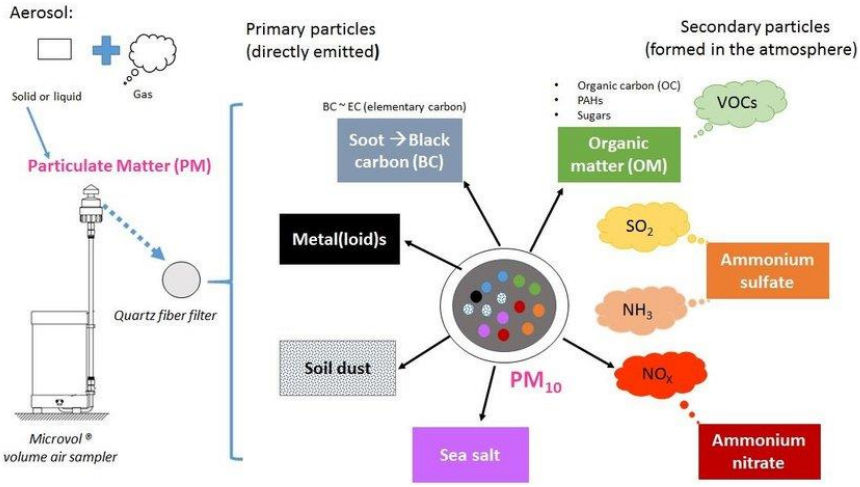

Figure 3.2: The average composition of PM is reported[10].

3.1.4 Atmospheric residence time and removal of PM

The atmospheric residence time τ of an aerosol is defined as the average time it spends in the atmosphere as a mutual result of the processes of formation/production against those of removal. Particulate Matter is basically removed by two main pathways i.e. respectively wet (which includes rain, snow, hail and fog) and dry deposition (basically particles precipitation caused by gravity) which are responsible of 20% and 80% of particulate[11]:

Dry deposition: it is the process in which the particulate falls to the ground because of the effect of the gravity when the velocity and the turbulence of the wind decreases. This velocity of removal depends on Stokes law: $v_s = \left(d_p^2 \rho_p g\right)/18\eta$ In which d_p is the granulometry of the particulate, ρ_p is the density, g is the gravitational acceleration, and η is the viscosity of the air. It holds for coarse particles. Instead, fine particles are aero

transported by turbulent diffusion within atmospheric circulation motion it is removed from the air streams by impaction on surfaces/obstacles during transport. Ultrafine particles disappear by means of high frequency collisions leading to the formation of intermediate particles such as Aitken and accumulation modes. Finally, it can be seen in this graphic how the time of residence depends on the size.

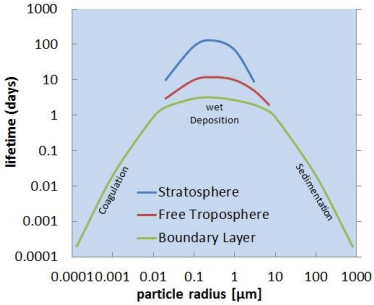

Figure 3.3: Correlation between particle radius and its lifetime[10].

- Wet deposition: it is split into: "in-cloud" and "below-cloud" processes. The in-cloud process consists in the fact that the droplets are formed around particulates called cloud condensation nuclei (CNN) when the air that contains water stream gets cooled or its humidity reaches 100%. This CNN have a size in the range 0,1-1µm[12]. They consist of hygroscopic particles especially from the oceans (Marine Spray allowing the condensation of the water vapour on them. Therefore, in cloud processes are very efficient in particle removal through cloud droplet formation. Once that the droplets have grown to a sufficient size to fall down as precipitation (or hydrometeor) they can intercept more aerosol particles while falling giving rise to extra particle removal defined as below-cloud.

There are other ways of removing particulate, for example impact with irregular, humid or electric surfaces or the impact with bigger particles[13].

To summarize the different ways to remove the particulate depending on the nature of each particulate; usually, natural particulate is coarse PM but tends to fall by precipitation, instead anthropically PM are fine particles and are less igroscopyc so, they are worse CNN.

3.2 Saharan Dust

In arid and semiarid zones, where precipitations are not frequent, the wind is responsible for the mechanical abrasion of the ground, producing coarse PM. The lack of precipitation in North Africa induce this region to be characterized by huge extension of sandy deserts which, once the sand is resuspended by the local winds, gets called Saharan Dust. This thesis consists in the analyse of filters that have been sampled in Sierra Nevada, Andalucía, Spain. The exact point is near to Pico Veleta and the University Hostel of Sierra Nevada. The site is limitedly affected by anthropic influences and they are vehicles reaching the SN and residential emission, plus pollution from the valleys below. The exact position coordinates are: 37.096 N, 3.387 W, 2550 m a.s.l

In this point even if the weather is continental, the precipitation is typical from a semiarid zone, therefore, very low. Moreover, in terms of geology this zone is called "Nevado-Filábride complex". This kind of geology is based on quartz, a material which is very resistant to erosion. Consequently, it will be theoretically difficult to have PM from this zone in the analyses.

Saharan Dust has a size distribution mainly in the coarse mode suggesting difficulties in long-range transport owing to the stokes law. However high energy wind regime over the African desert is responsible for huge dust resuspension and transportation up to several thousands of kilometres, sometimes reaching even the Alps and northern European countries. Regarding the chemical compound, Saharan Dust has a high content in clay materials (caolinite, gibsite, illite, smectite and paligorskite)[14]. In addition to that, quartz, carbonates and feldspate can be found as well as, in minor proportion but important to our research: gypsum, titan oxide and iron oxides like goethite and hematite, which is responsible for the reddish colour.

4. OBJECTIVES

- I had focused on different targets: To improve the reflectance techniques and the chemiluminescence method to improve the filter analysis and the quality data. This improvement was mainly focused on the reproducibility of this techniques.
- Set up an easy/cheap procedure to prepare Standards of hematite on quartz filters for the reflectance techniques.
- Finally, the main aim of this Final Degree Project is **the setting up and optimization of an integrated multi-technique method for characterizing Saharan Dust in PM from Sierra Nevada.**

5. EXPERIMENTAL SECTION

5.1 Sample analysis

The filters have been loaded with a weekly sampling and a high volume PM_{10} sampler since 8th of June until 11th of October 2016 (approximately19 weeks). These filters have a diameter of 13,6cm and are made of Quartz.

DRS UV-VIS data from the previous thesis[15] deserved some rethinking, mainly for one reason: the influence of the homogeneity of the filter along the entire surface had not been evaluated in the previous study. Therefore, in the present work, three square aliquots of 3.24 cm^2 from each filter (1.8 cm side) were cut, and the homogeneity of each filter was evaluated, as explained below. Then each portion was analysed as explained further below through different analytical techniques: DRS UV-VIS, FT-IR ATR, luminol-induced chemiluminescence. The aliquots of the filters were cut with scissors. Instead, this time die-cutting tools and a hammer have been used to cut the aliquots of each filter.

This method improves the cutting because it needs less interaction with the surface of the filter, and consequently it is cleaner, improving the final result.

Each cut aliquot had a square geometry of 1.8cm per side. For sake of analytical accuracy, 3 replicates of a field blank have been analysed too. A field blank is a blank that has gone through all the process (handling, transportation, and storage) that a filter passes through but without sampling. The sum of these 3 blank aliquots and the 3 aliquots of each one of all 19 filters makes a total of 60 samples to be analysed.

Afterwards, the analysis of all this obtained data plus the data obtained from Dra. Laura Tositti's student[16], and the ones given by the sample collectors like PM quantity, for example, will be correlated and analysed together.

The experimental part of all these techniques will be explained separately for each one, then the data processing of all these techniques will be explained, and finally the analyse of all data together will give us the final results.

5.1.1 Homogeneity test

While the filters are being cut, they need to be weighed. In the previous works with these filters the occasion to measure the homogeneity has never been felt. That is because, in Tullio's case[16], he just had 1 half filter to work with, therefore, with no repeatability. In Cingolani's case[15], the cutting was done with scissors, hence, the pieces where never the same size, therefore, no repeatability. With the die-cutting we got three exactly sized pieces for each filter. Then, we needed to apply a test of Fisher (F-test). Considering that blanks have a total homogeneity (as they have no particulate on its surface) its variance (Var B) has been compared with the rest of the sample variances (Var S) by an F-test. To apply this test, the F value needs to be compared with the calculated F:

- F value > F calculated → H_0 accepted → Var B not significantly (level of significance 5%) different than Var S → Homogenous

- F calculated > F valued → H_1 accepted → Var B significantly (level of significance 5%) different than Var S → Non-Homogenous

To calculate F, we just need to divide the variance between the samples of the same filter and the variance of the blanks. F value at a 5% of significance level, 2 degrees of freedom (DoF) for the samples, and 2 for the blanks (as there are 3 samples of each; DoF=n-1). The results of this test for each filter will be shown in section 6.1.

5.2 Reflectance Spectroscopy techniques

5.2.1 Ultraviolet-Visible Diffuse Reflectance Spectroscopy (UV-VIS DRS)

This reflectance technique is used as the first analytical technique, because it is conservative. It means that the samples do not need to be destroyed to be analysed. This is the only technique that has been used in this Final Degree Project having this characteristic. Theoretically, FT-IR ATR is a non-destructive technique. However, in our case, the contact between the crystal and the sample provokes the destruction or pollution of the sample. Consequently, the portion cannot be further analysed.

The specific aim of this technique is to find the exact peak of hematite and to find the relation between the colour of the sample and concentration of this iron oxide compound.

In this Project spectroscopic measurements of reflectance have been carried out irradiating the filters with a scan of UV-Vis radiation and measuring the diffused refraction generated by the samples at different wavelengths.

Moreover, it is known that this analytical technique is able to parametrize the colour of the analyte and obtain semi-quantitative information about the iron oxide minerals that are present in Saharan Dust[17] as reddish colour is characteristic of hematite (an iron oxide). The colour of an object can be obtained by this technique, as it depends on the diffusive reflection of the object in question. This phenomenon occurs when the object is enlightened from a light source. The object diffuses part of the incident

radiation by diffusive refraction reaching subsequently the eyes of the observer, which works as translators of the signal for the brain, that identifies the colour of the radiation. However, the colour perceived is not an object property, because it depends on many variables such as: source of light, light, optic behaviour of the object, eyes of the observer, processing of the radiation (brain), etc. Because it depends of all this variables CIE and International Organization for Standardization (ISO) establish that this data needs to be taken with normalized lightener D65 as light source. (ISO 11664-2:2007 (E) / CIE 014-2 S / E:2006)

Nevertheless, a mathematical model about colorimetric characteristics has been instrumentally defined in order to determine the colour of the object in a quantifiable and unambiguous way. An example of this colorimetric space is the one formed by CIE ("Commission Internationale de l'Eclairage" in English "Lighting International Commission") L*C*H:

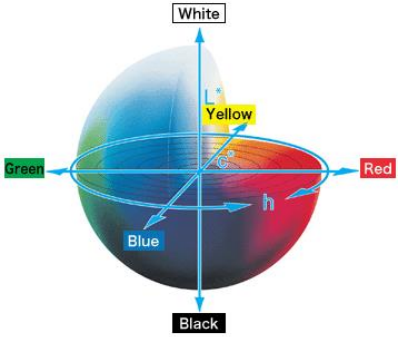

Figure 5.1: CIE L*C*H colorimetric model[18]

- Lightness (L): this value goes from 0 to 100. Where 100 is the whitest and 0 is the blackest.

- Chroma (C): explains the saturation which represents the intensity of the colour explaining how greyish the colour is.

- Hue (H): explains the tonality of the colour in degrees. Specifically, 0º represents the red colour.

As the hematite is responsible for Saharan Dust's reddish colour, this H component gives information about the quantity of this mineral in the sample.

5.2.1.1 Experimental procedure

The instrument has been used in single beam mode. The blank needs to be analysed first and then subtracted from the spectra of the PM samples. The reason why three filters have ben die-cut with 1,8*1,8 dimension is that the sample holder (Figure 5.2) has these same dimensions. As the holder is not in contact with the analysed side of the sample, this technique is non-destructive. One sample a time needs to be scanned.

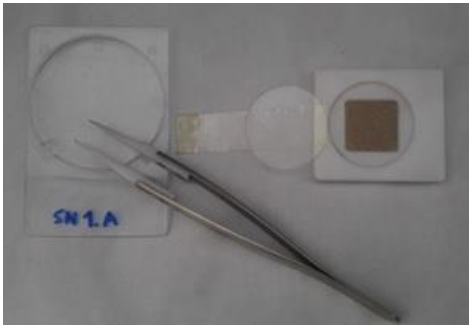

Figure 5.2: Sample ready to be analysed.

The Instrument has been programmed with the following parameters:

WAVELENGTH RANGE	From 380 to 780 nm
MEASURE CHARACTER	Reflectance rate (%R)
SCANNING VELOCITY	480 nm/min
SMOOTH	2 nm

Table 5.1 Parameters inserted to the Spectrophotometer

After this, one spectrum from each sample has been taken, as there are 3 samples of each PM filter, 19 filters plus the blank, that is 60 measures. No different measures from the same sample have been taken, since[15] C. Cingolani did that and the result was very similar for the same sample, so the result would hardly improve.

5.2.2 Fourier Transform Infrared Spectroscopy with attenuated total reflection Infrared spectroscopy transformed to Fourier in attenuate total reflectance (FT-IR ATR)

This is the second technique described in this Final Project which is able to provide the fingerprint of the functional groups of PM components sampled on active in the IR spectroscopic range.

5.2.2.1 Experimental procedure

The main advantage of this technique is that it does not need a special preparation of the PM sample collected on a quartz membrane which is analysed as it is. The die-cut piece just needs to be larger than the crystal (2 mm wide). In this case the diameter of the die-cutting tool used was 5mm. In order to prevent contamination of the sample and the consequent risk of producing an analytical artefact, handling of the sample is very critical especially when sample is put in contact with the ATR crystal tip.

After that, the instrument records the reflectance data from 4000 to 400 cm^{-1}, at a spectral resolution of 4 cm^{-1} with 64 scans rates. 60 samples were analysed according this procedure.

5.3 Luminol-dependent Chemiluminescence

This emission technique has also been used previously for PM filter analyses, not with Sierra Nevada but with filters from polluted areas in Italy. Unlike UV-Vis spectrometry, this technique is destructive. For this reason, an 8mm diameter circle has been die-cut and analysed for each sample.

The aim of this analysis is to obtain a semi-quantitative information about the Reactive Oxygen Species (ROS) a parameter associated with the potential toxicity of PM. ROS, include for example the radicals O_2*-, *OH, *OOH; they are oxidizing species able to trigger impairment and damage in living cells[1]. The method was tested herein in order to

investigate if Saharan Dust may reveal some bioactivity as a result of its content in submicron silica and or of its iron oxides.

5.3.3 Experimental procedure

The experimental procedure consists of preparing the 96-well plate for the analyses. In order to do this, samples need to be cut with the exact size of the well of the plate, i.e. a circle with a diameter of 8mm. Instead of using a punch, we used the 8mm diameter die-cutting tool to cut the sample. The aliquots in this way are regular and comparable and differently from past experiments, fits perfectly the well once pushed by an 8-diameter plastic tub directly to the bottom. The increase in the repeatability can be seen by the comparison of this 2 graphics (Figure 5.3) of the analyses by both methods of filters taken in Monfalcone during 2015:

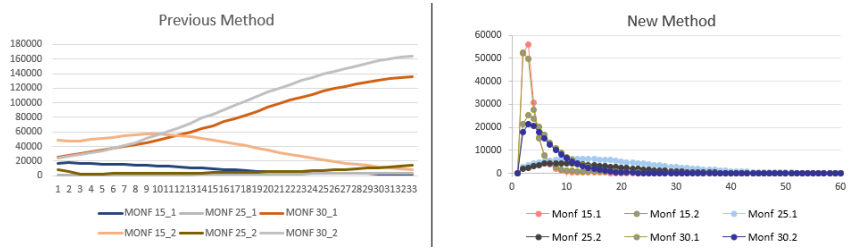

Figure 5.3: Comparison between graphics from chemiluminscence by the previous method and the improved method. The samples which are exponed have been selected randomly from all 23 filters, and it can be seen 2 repeats of each sample.

Comparing the data obtained before and after this experimental optimization, the following results emerge:

- Repeatability increases.
- Kinetics is closer to expected behaviour of the luminol method
- A maximum is found as a result of the technical improvement introduced in my thesis

5.4 From qualitative to quantitative analysis: Home-made resuspension system

The lack of certified filter standards causes the need to process the data obtained in a qualitative manner, without obtaining quantitative information. This fact led to the design and assembly of a home-made instrument capable of generating a filter-based standard for a quantitative approach, whose behaviour has been explored through an experimental design (Design of Experiment - DOE).

Both UV-Vis DRS and FTIR-ATR are generally used for qualitative purposes. In order to optimize their use a quantitative approach needs to be developed which can be done in two different ways, i.e. using targeted or untargeted methods. The untargeted approaches allow examining sample fingerprints, acquired by the use of spectroscopic, spectrometric or chromatographic techniques, in a holistic way and without the identification and quantification of specific and characteristic chemical species. Instead, targeted methods require the availability of suitable calibration standards prepared with the same sample geometry/presentation and quali-quantitatively known composition with the aim of the identification of specific and characteristic chemical species.

In the case of my thesis it was necessary to produce a series of synthetical filters depositing an accurately defined concentration of Hematite on a quartz membrane similar to the environmental PM samples studied. This method would be useful for the elaboration of a calibration curve for the hematite signal as a function of concentration to be used for both the reflectance spectral techniques used in this work. To start, the Project has focused on getting the standards of hematite for the UV-Vis diffuse reflectance spectroscopy and for the FT-IR ATR. For the first technique, Barium Sulphate ($BaSO_4$) and Magnesium oxide (MgO) are the only useful solids solvents the hematite can be mixed with. This fact is because of its low UV-Vis reflectance.

5.4.1 Resuspension system assembly

This assembly consists of a vacuum pump, a filter holder, several plastic tubes for the connection and a 25 ml Kitasato flask, used as a dust resuspension chamber. During air insufflation, the flask has been continuously kept under vibrational stirring to improve its homogeneity during the resuspension. The picture in Figure 5.4 reports the assembled experimental set up:

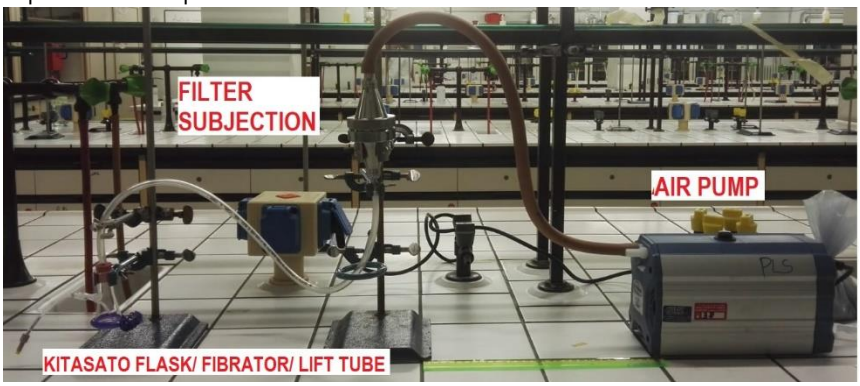

Figure 5.4: Resuspension system assembly

The flask was modified by connecting the side arm not perpendicularly to the flask axis as usual, but at a certain angle, in order to maximize the suction effect of the air stream on the resuspension of heavier particles and therefore allowing the collection of particles on the filter downstream the flask independently on the particle size, for a better simulation of PM size distribution.

5.4.2 Study and pre-optimization of the variables

To understand the way this assembly works several variables such as the time of suction, amount of powder in the chamber and composition of the mixtures prepared have been considered. The deposition on the filter was studied as a function of the listed parameters. To evaluate the homogeneity, a visual test was submitted to 10 people:

The test relies on different aspects. It was done just for people who has a connection with chemistry. Homogeneity in terms of quantity meaning was explained before the test: homogeneity is the quality or state of being of a similar kind or of having a **uniform structure** throughout. After that the less and the more homogeneous filters were fixed from PhD student Pietro Morozzi and me following the definition of homogeneity, in order to help the evaluator to understand what is intended by uniform structure. The evaluators review the rest of the filters with marks from 1 to 5 as explained. In this way the results of the test improved its repeatability between marks from different evaluators

The following filters were the most homogeneous filter obtained after the analyse with the mixture proportion and the variables applied for the experiment:

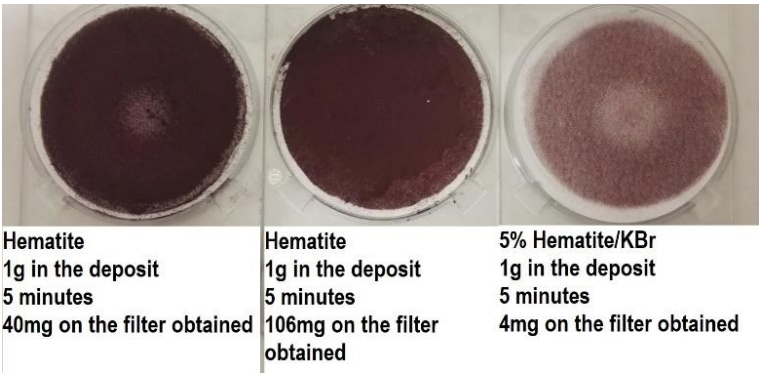

Figure 5.5: Filters obtained during the optimation tests of the resuspention system assembly

In 2 of them, we can see that in the middle of the filter there is an area with no dust. This is the likely effect of having a tube before the filter instead of a wider resuspension chamber. It is to note that for the spectral analysis conducted only an aliquot of the filter is actually necessary, so even if the deposit is actually not always perfect at least some areas are homogeneous enough for subsampling.

To analyse all these variables together, a design of experiment (DOE) test has been applied in the section 6.5.

6. DATA ANALYSIS: RESULTS AND DISCUSSION

6.1 Homogeneity

The data obtained by the Fisher test for each filter are showed in appendix 1.

As explained in point 5.1.1, what this test actually means is that if F calculated is higher than F value, the variance of the samples of the filter is significantly different than the variance of the blank[19]. It can be considered that the blank is perfectly homogeneous. Then if the variance of the artificial filter sample is the same as the blank variance, the filter can be considered homogeneous.

Most of the artificial filters gave F's ranging between 1 and 19, showing acceptable homogeneity. According to the outcome of the test applied filters SN1, SN16 and SN14 were discarded as F data obtained showed was higher than F value. Moreover, SN14 has an extremely high F. That will probably mean that one of these samples is an outlier in terms of quantity.

6.2 UV-VIS Spectroscopy (UV-VIS DRS)

6.2.1 Hematite signal obtention

In this section the aim will be to find the hematite signal of the samples. Hematite is a type of iron oxide (Fe_2O_3) that has an important relation with the colour of the samples. Another portion of the same samples was studied by[15] [Cingoliani C. and Tositti L., 2018]

so the pre-processing data will follow the same steps. After applying the data treatment hematite peak have a wavenumber of 535nm[20].

6.2.1.1 Kubelka-Munk (KM) remission function

Raw data is not suitable for the quantification of the hematite through its reflectance, because there is not a notable peak, the raw reflectance signal obtained was converted using the Kubelka-Munk remission function[21]. This function relates the diffusive reflectance (R), the absorbing coefficient (K) and the dispersion coefficient (S) as follows[29].

$$K/S = (1 - R_\infty)^2 / 2R_\infty \equiv F(R_\infty)$$

This function is only valid if the following approximations are assumed[22]:

1. The sample has a surface which is flat, and its extension is significantly larger than its thickness.
2. The sample is homogenous.
3. The scattering of the sample is random and isotropic.
4. The interfering light is null.

What needs to be homogeneous is not the whole filter, but the small area where the beam is focused, which is an approximation.

The result after this pre-processing data is the spectrum in figure 6.1.

In this graphic it can be seen that the hematite peaks are still hardly detectable being represented by a slightly perceivable decrease in Y axis ($1-R^2/2R$) at around 570-580 nm que to absorption by hematite itself. Therefore, another data processing needs to be applied.

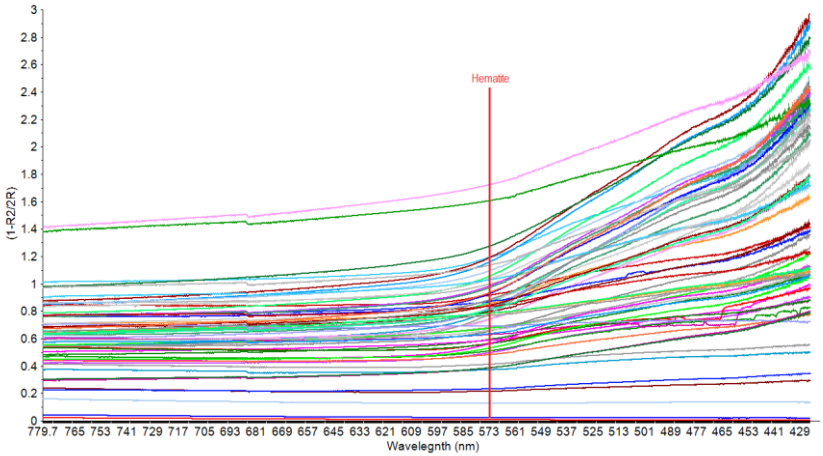

Figure 6.1: All samples with the Kubelka-Munk processing.

6.2.1.2 Second derivative processing

In order to obtain a useful spectral data with a clear hematite peak to work on, Savitsky-Golay 2nd Derivative function can be used owing the effect of this pre-processing that can be seen in figure 6.2. This function has many objectives:

- Remove background drift due to scattering.
- Resolve adjacent peaks.
- Because of Savitsky-Golay filter, it improves spectral resolution[22].

Moreover, the Savitsky-Golay filter is a digital filter which can be applied to smooth the data, increasing the signal-to-noise ratio without distorting the signal.

To provide an example of the function of this pre-processing, Figure 6.2 can help.

In this work, the Savitsky-Golay 2nd Derivative has been applied using a 4th polynomial grade, function that better fits with the selected 301 points that are used to obtain the spectral (150 points defined at the left of the central point, and 150 at the

right). This function produces a remarkable improvement in the spectral data of hematite (see Fig 6.2).

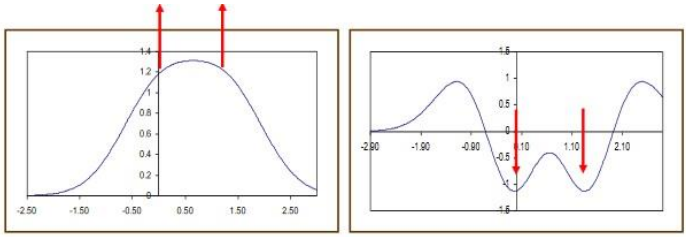

Figure 6.2: On the left non-derivated spectrum. On the right 2nf derivative spectrum[23].

The obtained plot is:

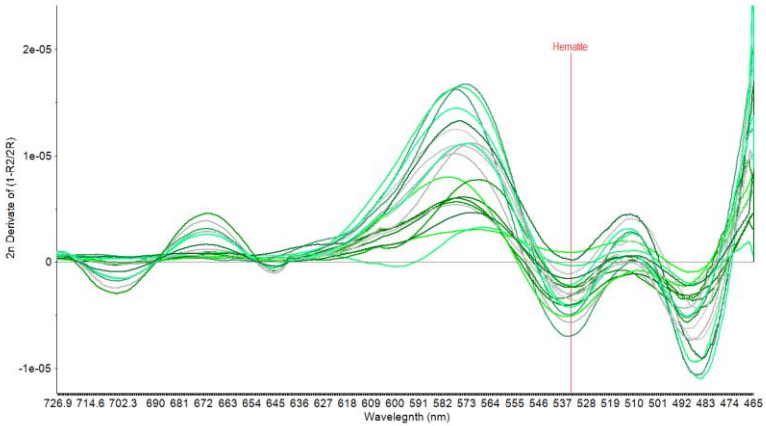

Figure 6.3: Savitsky-Golay 2n Derivate of the Kubelka-Munk remission function.

6.2.2 Hematite signal quantification

For quantitative analysis purposes the processed signal needs to be integrated. First, the baseline of the pick is plotted, and the total area of the peak is obtained by

integration. As said in section 6.2 this peak is at wavenumber 535nm[20]. The exact hematite peak' areas are showed in Appendix 2.

6.2.3 Colourimetry

Colorimetric data (Appendix 3) is directly obtained by the Spectrophotometer with no needs of data pre-processing.

As already seen in figure 5.1 the chroma (Cab*) is linearly correlated to hematite concentration, as this iron oxide is the responsible for the red colour in the Saharan Dust samples. Instead, hue (hab*) is inversely proportional to the red colour and then, to hematite concentration. Then, hematite can be explained by both coordinates of colorimetric (Cab* and hab*). As 0º of hue represents the tonality of the colour red, it is inversely correlated with hematite but the R^2 is higher than the correlation with Cab* which means that is more explicative of the colour that comes from the hematite. Results obtained are reported in Figure 6.4:

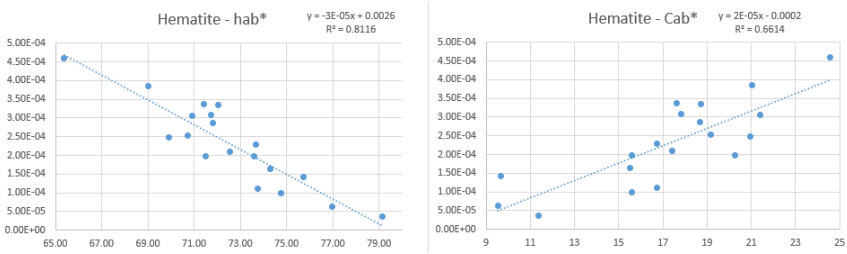

Figure 6.4: Graphic where can be seen the explained correlation between hab*-Hematite and Cab*-Hematite

6.3 Infrared Spectroscopy (FT-IR ATR)

6.3.1 Obtained data

In appendix 4 the FTIR-ATR spectra for the 60 PM samples and blanks analysed is reported.

The lowest spectra are those from the filter blanks and the sample SN4.B. Blanks will be treated separately, but they will not be subtracted from the rest of the samples. That is for different reasons:

- First, to subtract the blank is not important because the important band in this report is the hematite's signal. Which is not a chemical specie present in the blank.
- FT-IR ATR has an attenuate beam. This provokes that the beam does not penetrate into the filter, so the band of the blank should not be analyses in the samples[24].
- For the correlation analysis, it makes no change to subtract or do not the blanks signal. The blanks have a Quartz huge band around 1000cm^{-1}.

6.3.2 FT-IR ATR Data treatment

6.3.2.1 Multiplicative Signal Correction (MSC)

Multiplicative signal correction (MSC) is a relatively simple processing step that attempts to account for scaling effects and offset (baseline) effects[25]. The correction consists of regressing a measured spectrum against a reference spectrum and then correcting the measured spectrum using the slope (and possibly intercept) of this fit. As every filter sample has a different chemical matrix, an MSC was applied to the triplicates of each filter sample. The procedure generates a corrected spectrum as depicted in figure 6.5.

In this plot concerning only part of the samples (as all samples in the same plot would create confusion to the observer), two different things can be observed:

- Again, as with UV-Vis spectroscopy, SN3 and SN12 are the filters with a highest signal.
- SN4.B has a plot that seems different than the rest of the filters.

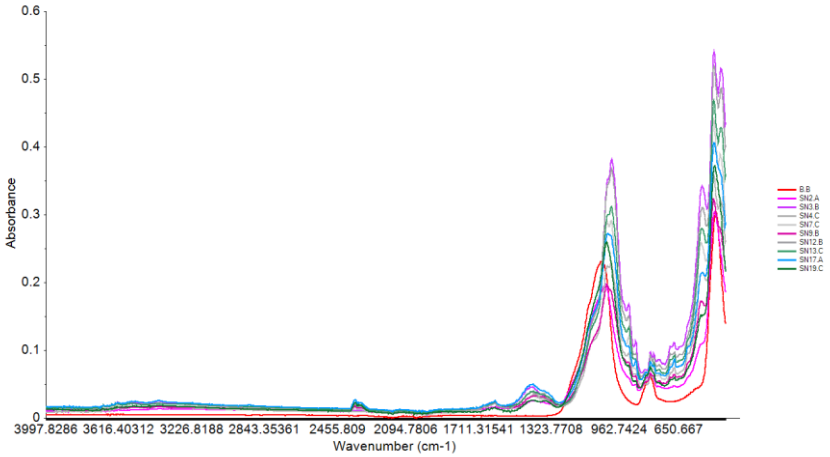

Figure 6.5: Plot Abs – Wavenumber (cm^{-1}) after applying MSC pre-processing for each filter.

6.3.2.2 Principal Component Analysis (PCA)

The corrected spectra data absorbance vs wavenumber with every sample was subsequently subjected to Principal Components Analysis (PCA) with two basic aims:

- Look for the outlier's samples in this technique.
- Obtain the most explicative variable, i. e. the most relevant wavenumbers of the entire spectra.

PCA is a statistical technique that converts a set of observations of possibly correlated variables into a set of linearly uncorrelated variables called Principal Components by using an orthogonal transformation[26]. This method substantially reduces the number of observations by describing it with PC's. PC1 is always the variable that accounts for the majority of the variance.

PCA can give information about the samples and the variables:

Usually, as far as variables are concerned, PCA is used to know:

- Which variables describe better the difference between samples.
- Which is the contribute of each variable to describe an observed difference.

- Which variables are cross-correlated.

As for the samples, it enables the detection of sample patterns and more importantly, it can be used to detect outliers.

We will use PCA for two reasons: first it will show the outliers, and then the most important variables (wavenumbers) will be taken to define the samples, so the variables that give more information about the filters will be selected.

Outlier identification and selection of the most explicative variable of the mathematical model

First, it will be shown the graphic of Hotelling T^2 – Q residuals for PC1 (Figure 6.7) that is just a different way of applying the F test[27]. This graphic has been drawn taking the 5% of significance level.

We can observe in this plot that SN4.B is clearly an outlier for the model of PCA created. Moreover, blanks are clearly almost out of the significance which is considered to be characteristic of a given population of data. SN3 is also far from the rest of the dataset, because it is clearly larger than the rest. The model is then recalculated after discarding sample SN4.B.

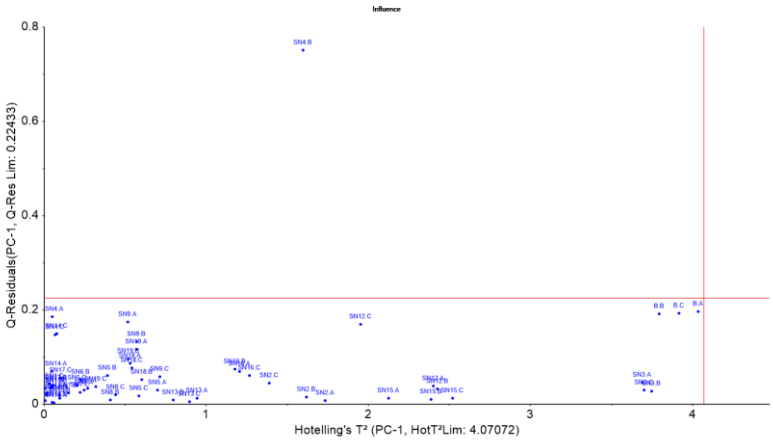

Figure 6.6: Hotelling T^2 – Q-Residuals for PC1

At this stage the model output allows to assess **which are the most significant variables.**

The PCA yields two principal outputs.

The SCORES PLOT: Which shows the contribution of PC for each sample.

The LOADINGS PLOT: Which shows to what extent each variable contributes to PC's.

The loading plots (for example the PC1 Loading reported below) reveals that the model yields 3 PC's: (PC1 ≈ 91%, PC2 ≈ 7%, PC3 ≈ 2%) explaining ≈ 100% of the system variance. This 3 PC have been used to select the most explicative variables for each component.

Afterwards Loadings plot will be used to point out which variables are statistically significant. As an example, the loading plot for PC1 is reported. This plot needs to be analysed for the first three PC.

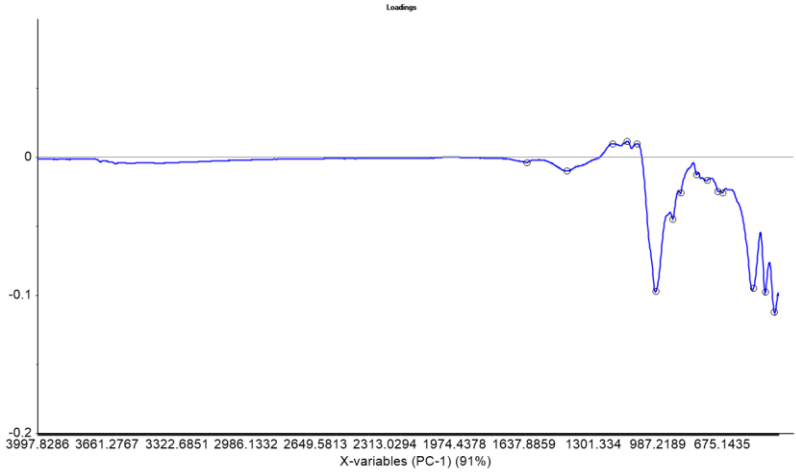

Figure 6.7: Loadings of PC1 principal variables selected

Variables with high Loading values in absolute terms for each one of the PC are previously selected. Then, the selected variables are very less in comparison with the starting variables. As the selected variables are the most explicative, the mathematical model is equally explained but with a lower number of variables. The number of selected variables is 24.

Hematite peaks identification

To study which variables hematite depends on, a standard portion of pure hematite has been analysed by FTIR-ATR. This standard has been obtained by means of the resuspension system explained in point 5.4. Specifically, it is the filter shown in the middle in figure 5.5. Therefore, this standard includes the filter signal, and can be compared with the rest of samples.

Figure 6.8 report the spectra of the artificial standard of pure hematite and of one of the PM samples herein analysed as an example. Differently from PM samples characterized by huge amount of Saharan dust, in the standard the quartz band has a very small intensity. Instead both peaks of hematite coincide with the PM sample both in

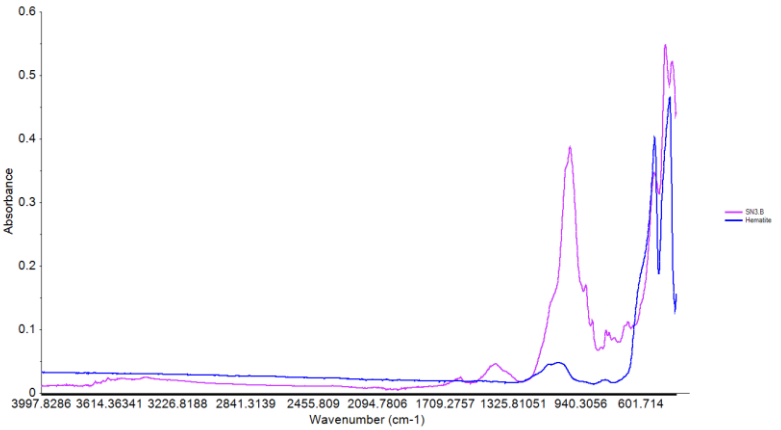

Figure 6.8: Plot about the comparison between Hematite and sample SN3.B Absorbance versus Wavenumber (cm^{-1})

terms of intensity and wavenumber. As previously described hematite peaks are found at 522cm^{-1} and 436cm^{-1}. The first peak has been selected previously as an important variable of the samples. But 436cm^{-1} has not been selected, probably because the matrix makes the peak shift of some inverse centimetre. Then, the selected variables which are closer to the hematite standard second peak are 446cm^{-1} and 420 cm^{-1}, plus the 522cm^{-1} already selected. These 3 variables will be informative about hematite concentration.

6.4 Luminol-dependent Chemiluminescence data processing

As previously described, samples of PM were analysed in triplicate. From the chemiluminescence spectra obtained, the peak value of each sample is selected, and

then the average for the sample replicates is calculated. To make the data more informative, the Activity (A) for each filter has been calculated. This is the difference between the sample (S) and the blank (B) in percent. Then:

$$A(\%) = {}^{(S-B)}/_{B} \times 100$$

Obtained Activity is reported in Appendix 5.

The values for filters 4 and 13 have been marked in red, to show that they have a relative error larger than 25%. In order to point out the existence of outliers within the sample triads, the Limit of Detection (LoD) of the method has been calculated first:

$$LoD = B_{SD} \times 3$$

In which B_{SD} is the standard deviation of the statistical population of the blank.

LoD can be used to see if a sample is significantly different from the blank or not (in this case, at the 95% confidence level). If the difference between the sample and the blank is lower than LoD, the sample signal is not significantly different from the blank. In this case, as expected, samples SN4.B and SN13.C are not significantly different from the blank.

To understand if this samples are outliers, they need to be compared to the rest of samples of the same filter:

SAMPLE	ACTIVITY
SN13.A	-42%
SN13.B	-41%
SN13.C	-24%
SN4.A	-30%
SN4.B	-7%
SN4.C	-29%

Table 6.1: Possible outlier samples.

Both SN4.B and SN13.C can be taken as outliers and discarded from the means obtained.

By this emission spectroscopy technique, the maximum obtained signal is for the filter SN4. This result is different than obtained results in reflectance techniques (UV-Vis and FT-IR ATR). However, the filter SN3 (which had the highest signal in these techniques) signal is the 2nd filter in terms of ROS emission by chemiluminescence. These results will be correlated in point 6.6 with the ion composition analyzed by Ion Chromatography[1], and the rest of data obtained in this report, in order to understand which of the ROS substances in the filters can be more important for the chemiluminescence signal.

6.5 Design of Experiment (DOE) about the dust resuspension system

The resuspension system is a home-made assembly that was made in this thesis in order to create standard filters of hematite. With the aim to understand the assembly behaviour for the setting up of hematite standards, a Design of experiment (DOE) was used. DOE is a chemometric technique that allow to create a matrix of experimental tests, for study and optimize a system. Therefore, in this thesis, this approach was used to explore the behaviour of the home-made resuspension system for the standard creation through the definition of a low number of experiments obtaining the maximum information about the assembly[28].

In particular, to compute a DOE two kinds of variables must be defined previously: the predictor variables, which are variables that define the behaviour of the instrument, and

the response variables, which are variables that define the final result of the experiments. Specifically, in the case of this thesis have been defined:

- 3 Predictor variables: Weight/weight percentage (%$_{w/w}$) of hematite, quantity of the mixture in the flask and duration of the resuspension experiment.
- 2 Response variables: Quantity of mixture on the filter and homogeneity.

The DOE, once predictor variables are defined, creates a dataset with the experiments that need to be done. Once the experiments are performed it is possible to calculate the response surfaces, which are the graphic representations of the response variables inside the surface defined by the predictor variables.

In particular, in this work, a two level (the maximum and the minimum of each predictor variable) plus a central point (average of minimum and maximum of both variables) full factorial design with two factors (quantity of the mixture in the flask and duration of the resuspension experiment) was performed. Therefore, the surface was a square (Figure 6.9). This operation was repeated for 6 different %$_{w/w}$ of hematite (as described below) and 6 surfaces were concurrently investigated[28]. If every surface needs to be explained with 5 points, it is a total of 30 experiments to perform.

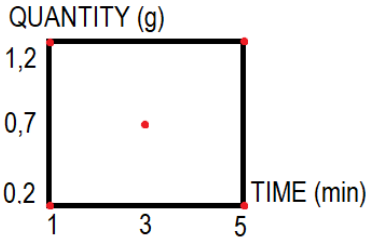

Figure 6.9: Mathematical surface for each analysed mixture. The points in red are where the analyse is done.

The limits for each response variable shown in Figure 6.9 and described below have been selected after many empirical tests with the assembled instrument, with the aim to reproduce the general features of the analysed PM filter samples: proportion of around 1%$_{w/w}$ of hematite, around 20mg of mixture on the filter, and the best homogeneity as possible. Then the limits of the variable are fixed as:

- Quantity of Mixture: Minimum: 0,2g; Maximum: 1,2g; Centre (average of maximum and minimum for both variables): 0,7g
- Time: Minimum: 1min; Maximum: 5min; Centre: 3min
- Mixture goes from 0% to 20% augmenting 4% each time. A square study for each mixture.

6.5.1 Doe obtained information

As explained, an experimental surface region was defined by the predicted variables and their extremes, in this way the behaviour of the experiment is understood in this region. The response variable points which were looked to obtain were the 20mg of mixture deposited on the filter with the highest homogeneity as possible. However, this point is out of the obtained surface of response. Then this analysed surface can only be used to understand the general behaviour of the resuspension system.

DOE has been studied with Unscrambler 9.7. These are the obtained plots

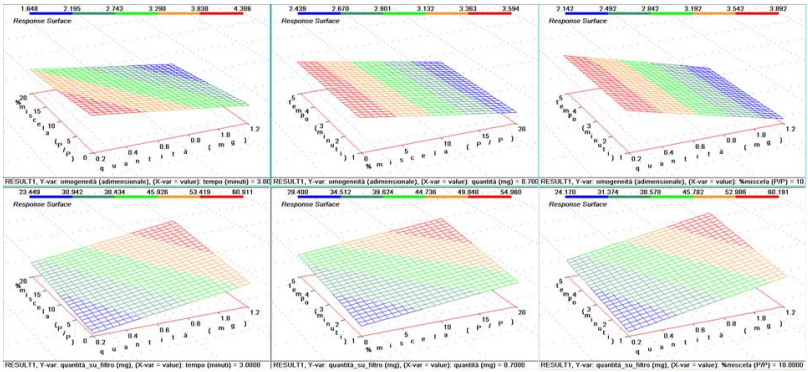

Figure 6.10: The plots on the top explain the Homogeneity and the plots on the bottom explain the quantity on the filter. From left to right the axes exaplain: Quantity vs Mixture, Mixture vs Time, Quantity vs Time.

All these plots have an R^2 too low. It varies from 0.45 to 0.65. Then the data analyse cannot be specific, but it needs to be used just as a general behaviour:

6.5.2 DOE Data analysis

Quantity of dust deposited on the filter:

Variables	Behaviour
Quantity & Time	Direct with both. The less Q and less T, less dust is deposited on the filter.
% of Hematite & Time	Direct with both. The higher % of Hematite in the mixture and more time of dust resuspension, more dust can be found on the filter.
% of Hematite & Quantity	Direct with both. The more Q and % Hematite, the more deposition.

Homogeneity:

Variables	Behaviour
Quantity & Time	Inversely correlated with Quantity and no effect of Time.
% of Hematite & Time	Inversely correlated with % of Hematite. Time has a reverse effect until 10% of Hematite, then time has no effect again on the homogeneity.
% of Hematite & Quantity	Inversely correlated with both.

Table 6.2: Summary of the results obtained by the DOE resuspension system

6.6 Total Spearman Correlation Analysis

At the end of the experimental work conducted in this thesis it was possible to provide the 19 weekly samples of PM from Sierra Nevada with series of new quantitative data concerning specific chemical parameters associated with its complex composition. In

order to study their association with chemical compounds previously determined in this lab, a Spearman's rank Correlation analysis was performed. Index of Spearman Correlation (r_s) is a statistical measure of the strength of a linear relationship between paired continue and aleatory data. It varies between -1 & +1. Then, the minimum r_s needs usually to be |0,6| or |0,7|[29] to consider that there is a correlation between 2 paired data. However, in this case, we have taken |0,8| to assume that the correlation is very strong, and |0,7| to assume that it is correct If the Spearman Correlation is negative, it means that the relationship is inverse.

Spearman Correlation watches the relationship between two paired data that follow a monotonic function. It means that, while its independent variable increases, the dependent variable always increases or decreases[29]. It can be easily understood with the figure 6.1.

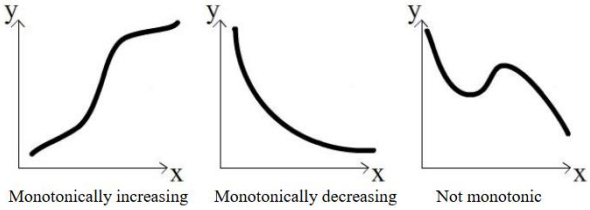

Figure 6.11: Example of monotonic and not monotonic function[29].

For the Spearman correlation analyse every data about the Sierra Nevada Filters has been used. In appendix 6, tables of Spearman correlation are reported. In these tables the following data is marked with the same colours as below. That is:

Temperature, pressure, and PM_{10} (Measured data by Granada University)

Ionic composition (Na^+, NH_4^+, K^+, Mg^{2+}, Ca^{2+}, Cl^-, NO_3^-, Acetate, Oxalate, Formate, and Methanesulfonate[1].

Hematite UV-Vis signal (Normalized data). and colour data obtained from the Spectrophotometer.

Maximum Chemiluminescence on point 6.3. (Normalized data).

Variables selected with the PCA from the FTIR-ATR analysis, with a special attention on hematite point selected. (Normalized data).

Table 6.3: Legend of data included in the Spearman correlation for the section 6.6.1 Data analysis and its tables.

6.6.1 Data analysis

In Appendix 7. The complete Spearman correlation table is reported.

Correlation with PM_{10}

PM_{10} is the mass divided by the volume of air pumped through the filter. It was determined at Granada University.

The degree of correlation is given by the value of the R i.e. the correlation coefficient produced by this model. First, there is a strongly direct correlation of PM10 with Ca^{2}+ (+0.76) and SO_4^{2}- (+0.78). This result can be explained by a significant quantity of gypsum (CaSO4·2H2O), that represent a Saharan Dust component as previously described in section 3.2.

Then the correlation with the colour data means that most component of the PM_{10} is Saharan Dust, because it is directly correlated with hematite signal obtained by UV-Vis (0.71), also correlated with Cab* (+0.84) and inversely correlated with hab+(-0.91). In section 5.2.1 is explained that these data are representative of the reddish colour of Saharan Dust.

There is a direct correlation between PM10 and the chemiluminescence signal, even if the correlation index is not very high (+0.69).

Finally, the correlation with the IR variables is usually direct, it happens because the more PM_{10}, the more intense is the overall signal, but there is no difference on the shape of the plot.

Finally, the IR signal 522 cm^{-1}, the hematite Standard peak, is the one with the higher correlation (+0.81).

Hematite and Colourimetry

It has already been seen how hematite and colour data is correlated with weight and PM_{10}.

With this Spearman correlation it can be demonstrated what has already seen in figure 6.4. Hematite has a good correlation with Cab* (+0.79) and hab* (-0.82), characteristics of the reddish colour. Of course, the relation between Cab* and hab* is inverse (-0.94) as they describe the opposite kind of colourimetry.

Hematite, Cab* and hab* follow the same kind of correlation with most of data. However, hematite has no correlation with anyone of the ion concentration. Instead, Cab* and hab* have a direct and inverse correlation with Na^+, Mg^{2+}, Ca^{2+}, Cl^-, NO_3^-, SO_4^{2-}.

There is not a high correlation between hematite and Chemiluminescence signal. However, there is an inverse correlation with hab* (-0.73).

Finally, it needs to be specified that hematite maximum peak at IR data (522 cm^{-1}) is the wavenumber that has the highest correlation with hematite (+0.85), that is important because it means that we should be able to find the concentration of hematite if we improve the standard formation through the home-made dust resuspension system.

Chemiluminescence

Chemiluminescence peaks have an important correlation only with Ca^{2+} concentration (+0.78) this is the same result as [A. Ramkiran et al. 2017][30] saw with CaO, as they found that the chemiluminescence intensity increases 8 times with this oxide. Furthermore, [RIF 40] saw that at an increasing in the calcium concentration corresponds an increment of chemiluminescence signal. Then, the reason of this correlation is probably that the presence of Ca^{2+} improves the chemiluminescence signal. Moreover, the chemiluminescence signal seems to be correlated also with the oxidative anions like NO_3^- (+0.74), SO_4^- (+0.74), or acetate (+0.80), but their role in the luminol emission reaction it still needs to be deepened.

However, there is not a strong correlation with hematite (+0.66), neither with IR hematite absorbance bands, which means that hematite would seem not to have an important effect on luminol reaction, even if this hypothesis needs to be confirmed by the PIXE iron data.

There is correlation with none IR data.

Infrared spectroscopy

In this case most of correlations have already been analysed. Most of selected IR variables which are lower than 995cm^{-1} characterize the quantity of quartz/silica and iron oxides. Then, as a summary, these IR variables selected by the PCA loadings plot (section 6.3.2.2) have a good correlation with the PM_{10} as it increases the amount of quartz/silica and hematite. The same correlation happens with hematite signal and colourimetry: direct correlation with hab* and indirect (but higher in absolute terms) correlation with Cab+. It is important that variable 522cm^{-1} (hematite standard wavenumber) has the best correlation with hematite signal (+0.85) and with PM_{10} (+0.81). Then variables which are lower than 995 cm^{-1} are all mutually correlated.

7. CONCLUSIONS

At the beginning of this report there were 3 objectives that needed to be accomplished.

1. About the improvement of the spectrometric analysis of the Hematite:

✓ Sierra Nevada starting filters were tested for homogeneity. 3 of them cannot be taken as homogeneous filters. These are SN01, SN14 and SN16. Then, the portion used for the analysis carried out in this thesis are not characteristics of the entire filter in terms of quantity of dust.

✓ UV-VIS DRS data from a previous work[2] were improved and extended to colorimetric analysis, however quantitative analysis could not be achieved yet.

✓ Hematite specific FTIR ATR wavenumber was determined by analysing the hematite standard filter obtained from the home-made assembly. Moreover, semi-quantification of hematite concentration was carried out by the UV-Vis reflectance technique. The Spearman correlation between hematite data of both reflectance technique was high (+0.87).

✓ Finally, the last part of this work concerned the optimization of a method based on chemiluminescence for their determination, which have been achieved by the improving of repeatability of the method.

2. A method for preparing PM standards on a filter has been successfully set-up – the device based on a Kitasato flask, a filter holder and a pump has been tested for a single mineral component, hematite, relevant for the environmental PM10 samples from southern Spain investigated in this work, and the preparation of a pure hematite standard filter has been successfully. Moreover, the applied DOE test has been used to understand the general behaviour of this assembly, and the final conclusions are:

✓ Homogeneity decreases when quantity on the filter increases.

✓ Pumping time have a maximum in relation with response variables: after some time (not quantifiable yet) it has no effect neither on the quantity or on the homogeneity.

3. By the Spearman correlation some conclusions can be taken or confirmed about the multi-instrumental analysis:

✓ Variable 522cm^{-1} of the IR data is characteristic of the hematite concentration, as it is the most correlated with hematite data of UV-Vis and the colorimetry data, with PM_{10} and does not depend on the rest of chemical species.

✓ Maximum of chemiluminescence has the maximum correlation with acetate, which is not an important chemical species of Saharan Dust and it is not correlated with hematite. Then this emission technique can be used as complementary with the reflectance technique in a multi-instrumental analysis of PM_{10} filters.

In summary, the multi-instrumental method was optimized even if quantified data was not achieved yet, only semi-quantified data was obtained.

8. BIBLIOGRAPHY

1. Tositti L., **2018**, Clinical Handbook of air pollution-related diseases, ed. Springer

2. Bonasoni, P & Cristofanelli, P & Sandro, Fuzzi & Gobbi, Gian Paolo & Van Dingenen, Rita & Tositti, Laura & Balkanski, Yves. (**2003**). Ozone and aerosol correlation during Saharan dust transport episodes at Mt. Cimone. 5076.

3. Harrison R, Yin J. Particulate matter in the atmosphere: which particle properties are important for its effects on health? Sci Total Environ. **2000**; 249:85–101.

4. Brook RD**,** FranklinB, CascioW, et al. Air pollution and cardiovascular disease: a statement for healthcare professionals from the Expert Panel on Population and Prevention Science of the American Heart Association, Circulation, **2004**, vol. 109 (pg. 2655-71)

5. Dockery DW., PopeCA3rd, XuX, et al. An association between air pollution and mortality in six U.S. cities, N Engl J Med **1993**, vol. 329 (pg. 1753-9)

6. Heyder J., Portsendörfer J., **1974**. Comparison of optical and centrifugal aerosol spectrometry: liquid and non-spherical particles. Aerosol Science 5, pp. 387 – 400

7. https://www.dwd.de/EN/research/observing_atmosphere/composition_atmosphere/aerosol/cont_nav/particle_size_distribution.html Deutscher Wetterdienst, 05-11-18

8. Seinfeld J., Pandis S., **1998/2006**. Atmospheric chemistry and physics.

9. WMO (World Meteorological Organization), Scientific Assessment of Ozone Depletion: **2010**, Global Ozone Research and Monitoring Project–Report No. 52, 516 pp., Geneva, Switzerland, 2011.

10. Barraza, Fiorella. **(2017).** Human exposure assessment related to oil activities in Ecuador: from the air quality monitoring to the study of metallic contaminants transfer in the soil-plant continuum.
11. Poulida O., Schwikoski M., Baltensperger U., Gäggeler H. W., **1998**. Scavenging of Atmospheric constituent in mixed phase clouds at high-alpine site Jungfraujoch part III:
12. Molinaroli E., Masiol M., **2006**. Particolato atmosferico e ambiente mediterraneo - Il caso delle polveri Sahariane. Ed. Aracne.
13. K. Pye **1987**. Aeolian Dust and Dust Deposits.
14. Reiff J., Forbes G.S., Spieksma F.T.M., Reynders J.J., **1986**. African dust reaching Northwestern Europe: a case of study to verify trajectory calculations. Journal of Climate and Applied Meteorology 25, pp. 1543 – 1567.
15. Cingolani C., AA **2017-2018**. Ottimizzazione di una rapida metodologia analitica per l'individuazione di fenomeni di incursione di polveri Sahariane nel bacino Mediterraneo. Tesi di laurea in Chimica e Chimica dei Materiali, Università di Bologna (Tutor: Prof.ssa Tositti Laura).
16. Tullio S., AA **2016-2017**. Analisi tramite cromatografia ionica di aerosol atmosferico in un sito della Sierra Nevada, Spagna. Tesi di laurea in Chimica e Chimica dei Materiali, Università di Bologna (Tutor: Prof.ssa Tositti Laura).
17. Arimoto R., Balsam W., Schloesslin C., **2002**, Visible spectroscopy of aerosol particles collected on filters: iron-oxide minerals, Atmospheric Environment, Volume 36, Issue 1, Pages 89-96, ISSN 1352-2310.
18. https://www.konicaminolta.com/about/research/instruments/instrument_001.html, Konica Minolta, 11/12/2018
19. Torrent J., and Vidal Barrón, **2002**,"Diffuse reflectance spectroscopy of iron oxides." Encyclopedia of surface and Colloid Science 1 (2002): 1438-1446.
20. Sellitto V., Barrón Vidal, P. G., Salzano R., Colombo C. (**2008**). Uso della spettrometria di riflettanza diffusa (DRS) e bi-direzionale (BRF) per lo studio dei suoli vulcanici europei.
22. T. Afonso, R. Moresco, V. G. Uarrota, B. B. Navarro, E. da C. Nunes, M. Maraschin, M. Rocha, **2017**. UV-Vis and CIELAB Based Chemometric Characterization of Manihot esculenta Carotenoid Contents. Journal of Integrative Bioinformatics
22. D.N. Rutleg**, 2011**. Data Pre-processing. AgroParisTech
23. Andrew R Hind, Suresh K Bhargava, Anthony McKinnon, At the solid/liquid interface: FTIR/ATR — the tool of choice, Advances in Colloid and Interface Science, Volume 93, Issues 1–3, **2001**, Pages 91-114, ISSN 0001-8686
24. H. Martens and T. Naes, Wiley. **1900**. Multivariate calibration. Journal of chemometrics vol 4 441.
25. C.B. Crawford and G.A. Ferguson, A general rotation criterion and its use in orthogonal rotation, Psychometrika, 35(3), 321-332**, (1970)**.
26. J.E. Jackson and G.S. Mudholkar, Control procedures for residuals associated with principal component analysis, Technometrics, 21, 341-349 **(1979).**
27. Kendall, M. G.; Stuart, A. **(1973**). The Advanced Theory of Statistics, Volume 2: Inference and Relationship.
28. Montgomery, D.C. **(1997):** Design and Analysis of Experiments (4th ed.) Wiley.

29. I. Weir. Spearman Rank Correlation. http://www.statstutor.ac.uk/resources/uploaded/spearmans.pdf 24/12/18
30. Ramkiran, V. G. Mohan, P. Mishra, N. Padmavathy, 2018. Enhanced Chemiluminescence of Luminol by Metal Peroxides Nanoparticles. Chemistry of Advanced Materials 3(1) (**2018**) 16-22

9. ACRONYMS

FRESA: Impacto de las intrusiones de masas de aire con polvo africano y de masas de aire estratosférico en la Península Ibérica. Influencia de El Atlas, 2015 - MINISTERIO DE ECONOMIA Y COMPETITIVIDAD, Programa Estatal de I+D+i Orientada a los Retos de la Sociedad) - Proyectos EXCELENCIA y Proyectos RETOS - Involves among others the UNIVERSIDAD MIGUEL HERNANDEZ DE ELCHE as coordinator, the Universities of Granada and Bologna

UV-VIS DRS: Ultraviolet-Visible Diffuse Reflectance Spectroscopy

FT-IR ATR: Fourier Transform Infrared Spectroscopy with attenuated total reflection

ROS: Reactive Oxygen Species

PM: Particulate Matter

PCA: Principal Component Analysis

VOCs: Volatile Organic Compounds

SD: Saharan Dust

DoF: Degrees of Freedom

APPENDICES

APPENDIX 1: Test F; Homogeneity

N. Filters	F Calculate	F Value	Homogeneity
SN1	19.5266	19	NO
SN2	1.511596	19	YES
SN3	17.206	19	YES
SN4	1.442913	19	YES
SN5	6.410641	19	YES
SN6	13.5648	19	YES
SN7	3.709413	19	YES
SN8	23.10914	19	YES
SN9	9.736698	19	YES
SN10	10.85539	19	YES

N. Filters	F Calculate	F Value	Homogeneity
SN11	7.581173	19	YES
SN12	2.706685	19	YES
SN13	1.747613	19	YES
SN14	5343.439	19	NO
SN15	1.42885	19	YES
SN16	19.97817	19	NO
SN17	3.291951	19	YES
SN18	6.083122	19	YES
SN19	2.263302	19	YES

APPENDIX 2: Average of the hematite area for each filter

FILTER	AREA	FILTER	AREA	FILTER	AREA	FILTER	AREA
B	1.97E-06	**SN5**	2.53E-04	**SN10**	2.47E-04	**SN15**	2.47E-04
SN1	1.11E-04	**SN6**	3.07E-04	**SN11**	2.10E-04	**SN16**	2.10E-04
SN2	3.74E-05	**SN7**	3.37E-04	**SN12**	4.59E-04	**SN17**	4.59E-04
SN3	3.84E-04	**SN8**	1.97E-04	**SN13**	3.09E-04	**SN18**	3.09E-04
SN4	2.87E-04	**SN9**	1.64E-04	**SN14**	1.99E-04	**SN19**	1.99E-04

APPENDIX 3: Colourimetry Data

	L*	A*	B*	CAB*	HAB*
SN1	69.61	4.69	16.06	16.73	73.73
SN2	70.19	2.14	11.18	11.39	79.15
SN3	65.01	7.53	19.62	21.02	69.01
SN4	61.33	5.83	17.74	18.68	71.81
SN5	61.56	6.32	18.07	19.15	70.73
SN6	67.17	6.99	20.20	21.38	70.91
SN7	58.60	5.60	16.69	17.61	71.44
SN8	65.73	6.43	19.20	20.25	71.49
SN9	60.17	4.20	14.93	15.51	74.29
SN10	63.71	7.20	19.69	20.97	69.92
SN11	61.97	5.23	16.62	17.42	72.55
SN12	66.35	10.22	22.31	24.55	65.38
SN13	63.99	5.59	16.95	17.84	71.73
SN14	57.64	4.40	14.95	15.58	73.58
SN15	67.09	2.15	9.29	9.54	76.96
SN16	56.20	2.39	9.39	9.69	75.72
SN17	64.42	4.70	16.05	16.72	73.68
SN18	62.24	5.77	17.82	18.73	72.06
SN19	76.31	4.10	15.04	15.59	74.74

APPENDIX 4: Chemiluminescence signal in terms of Activity

FILTER	ACTIVITY	ε_R
SN15	- 80%	5.6%
SN2	- 75%	4.0%
SN19	- 68%	5.4%
SN16	- 67%	5.0%
SN1	- 65%	7.5%
SN17	- 59%	3.4%
SN12	- 58%	4.4%
SN8	- 57%	5.6%
SN9	- 55%	9.8%
SN18	- 54%	3.1%
SN14	- 53%	9.8%
SN6	- 47%	9.2%
SN5	- 46%	1.4%
SN13	- 41%	28.0%
SN10	- 40%	16.1%
SN11	- 40%	8.5%
SN7	- 38%	2.7%

APPENDIX 5: Graphic; IR row data of all samples

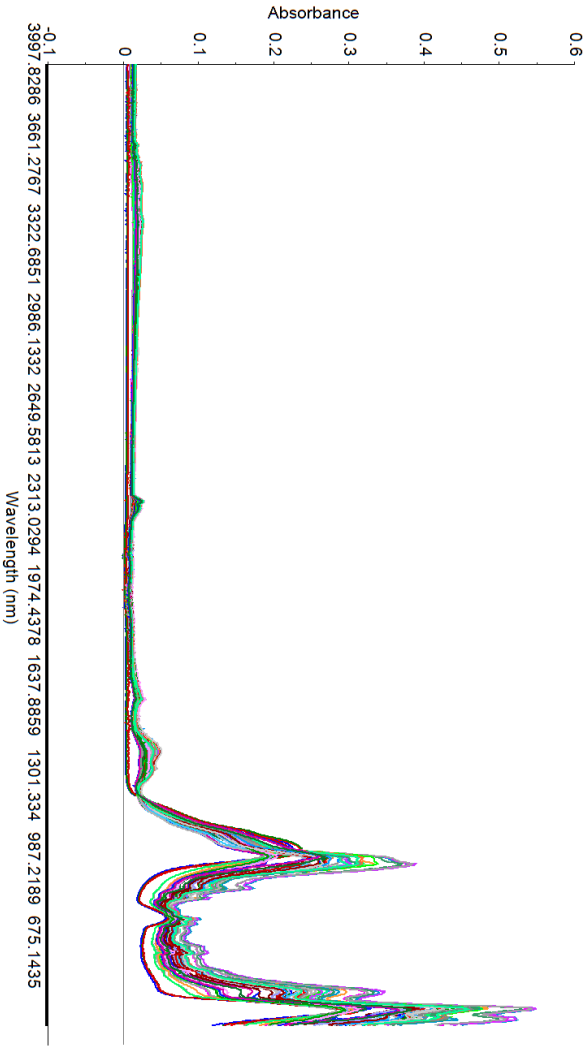

APPENDIX 6: Spearman Correlation; separated tables for each data

Sc > +0.8	+0.8 > Sc > +0.7	-0.7 > Sc > -0.8	Sc < -0.8

Legend: Colour depending on the Spearman correlation (Sc)

Variable	Correlation with PM10
Temperature	0.67
Pressure	0.39
PM10	1.00
Na+	0.65
NH4+	0.29
K+	0.66
Mg2+	0.80
Ca2+	0.76
Cl-	0.64
NO3-	0.69
SO42-	0.78
Acet	0.63
Form	0.34
Metsolf	0.15
Ox	-0.13

Variable	Correlation with PM10
hematite	0.71
L*	-0.08
a*	0.89
b*	0.84
Cab*	0.84
hab*	-0.91
Chem signal	0.69
2360 cm-1	-0.38
2342 cm-1	-0.34
1622 cm-1	0.22
1426 cm-1	0.51
1338 cm-1	0.17
1203 cm-1	-0.64
1173 cm-1	-0.36
1134 cm-1	-0.32

Variable	Correlation with PM10
1085 cm-1	-0.02
1065 cm-1	0.23
1032 cm-1	0.67
995 cm-1	0.76
912 cm-1	0.76
873 cm-1	0.71
798 cm-1	0.57
747 cm-1	0.65
694 cm-1	0.78
671 cm-1	0.72
600 cm-1	0.78
532 cm-1	0.78
522 cm-1	0.81
463 cm-1	0.76
447 cm-1	0.71
420 cm-1	0.80

PM_{10} Correlation with the rest of data

Variable	Correlation with Chemiluminescence signal
Temperature	0.61
Pressure	0.45
PM10	0.69
Na+	0.74
NH4+	0.18
K+	0.67
Mg2+	0.72
Ca2+	0.78
Cl-	0.36
NO3-	0.74
SO42-	0.74
Acet	0.80
Form	0.53
Metsolf	0.32
Ox	-0.41

Variable	Correlation with Chemiluminescence signal
hematite	0.63
L*	-0.43
a*	0.70
b*	0.64
Cab*	0.64
hab*	-0.73
Chem signal	1.00
2360 cm-1	-0.29
2342 cm-1	-0.28
1622 cm-1	0.24
1426 cm-1	0.23
1338 cm-1	0.08
1203 cm-1	-0.49
1173 cm-1	-0.38
1134 cm-1	-0.36

Variable	Correlation with Chemiluminescence signal
1085 cm-1	-0.09
1065 cm-1	0.17
1032 cm-1	0.46
995 cm-1	0.52
912 cm-1	0.53
873 cm-1	0.41
798 cm-1	0.41
747 cm-1	0.42
694 cm-1	0.55
671 cm-1	0.51
600 cm-1	0.55
532 cm-1	0.55
522 cm-1	0.57
463 cm-1	0.52
447 cm-1	0.48
420 cm-1	0.58

Chemiluminescence signal Correlation with the rest of data

Variable	hematite	L*	a*	b*	Cab*	hab*
Temperature	0.61	-0.10	0.56	0.60	0.60	-0.63
Pressure	0.41	-0.06	0.40	0.45	0.43	-0.44
PM10	0.71	-0.08	0.89	0.84	0.84	-0.91
Na+	0.66	-0.17	0.79	0.78	0.77	-0.71
NH4+	0.37	-0.41	0.16	0.11	0.11	-0.24
K+	0.38	-0.46	0.59	0.53	0.53	-0.60
Mg2+	0.57	-0.28	0.74	0.68	0.68	-0.73
Ca2+	0.58	-0.11	0.79	0.78	0.77	-0.73
Cl-	0.45	0.29	0.71	0.72	0.72	-0.59
NO3-	0.58	-0.31	0.82	0.77	0.77	-0.75
SO42-	0.58	-0.15	0.72	0.69	0.69	-0.71
Acet	0.61	-0.49	0.60	0.54	0.54	-0.66
Form	0.45	-0.44	0.33	0.31	0.32	-0.37
Metsolf	-0.07	-0.16	0.09	0.11	0.09	-0.09
Ox	-0.08	0.04	-0.16	-0.10	-0.12	0.21
hematite	1.00	-0.14	0.80	0.77	0.79	-0.82
L*	-0.14	1.00	-0.01	0.12	0.13	0.10
a*	0.80	-0.01	1.00	0.98	0.98	-0.97
b*	0.77	0.12	0.98	1.00	1.00	-0.94
Cab*	0.79	0.13	0.98	1.00	1.00	-0.94
hab*	-0.82	0.10	-0.97	-0.94	-0.94	1.00
Chem signal	0.63	-0.43	0.70	0.64	0.64	-0.73

Variable	hematite	L*	a*	b*	Cab*	hab*
2360 cm-1	-0.04	-0.21	-0.22	-0.24	-0.25	0.23
2342 cm-1	-0.03	-0.23	-0.20	-0.22	-0.23	0.21
1622 cm-1	0.49	-0.45	0.26	0.21	0.22	-0.27
1426 cm-1	0.55	0.06	0.55	0.55	0.56	-0.49
1338 cm-1	0.34	-0.26	0.22	0.18	0.19	-0.17
1203 cm-1	-0.58	0.20	-0.47	-0.43	-0.45	0.59
1173 cm-1	-0.33	0.37	-0.19	-0.14	-0.15	0.33
1134 cm-1	-0.30	0.39	-0.12	-0.07	-0.07	0.28
1085 cm-1	0.03	0.38	0.22	0.24	0.25	-0.10
1065 cm-1	0.31	0.33	0.46	0.48	0.49	-0.38
1032 cm-1	0.78	0.08	0.80	0.83	0.84	-0.79
995 cm-1	0.84	0.00	0.83	0.82	0.84	-0.85
912 cm-1	0.81	-0.10	0.79	0.76	0.78	-0.82
873 cm-1	0.78	0.07	0.78	0.77	0.78	-0.75
798 cm-1	0.67	-0.03	0.69	0.68	0.69	-0.68
747 cm-1	0.74	-0.04	0.71	0.69	0.71	-0.71
694 cm-1	0.83	-0.06	0.83	0.81	0.82	-0.85
671 cm-1	0.83	-0.02	0.81	0.80	0.81	-0.79
600 cm-1	0.84	-0.03	0.84	0.83	0.84	-0.83
532 cm-1	0.83	-0.07	0.81	0.78	0.80	-0.84
522 cm-1	0.85	-0.05	0.85	0.83	0.84	-0.87
463 cm-1	0.77	0.01	0.82	0.82	0.83	-0.84
447 cm-1	0.76	0.08	0.82	0.84	0.84	-0.82
420 cm-1	0.82	-0.05	0.85	0.84	0.85	-0.87

Hematite and colourimetry data Correlation with the rest of data